

Restricting Voltage Deviation of DC Microgrids with Critical and Ordinary Nodes: A Generalized Consensus Approach ^{*}

Handong Bai ^a, Peng Li ^b, Hongwei Zhang ^{b*}

^a*School of Electrical Engineering, Yellow River Conservancy Technical Institute, Kaifeng, Henan 475004, P.R. China*

^b*School of Intelligence Science and Engineering, Harbin Institute of Technology, Shenzhen, Guangdong 518055, P.R. China*

Abstract

Restricting bus voltage deviation is crucial for normal operation of multi-bus DC microgrids, yet it has received insufficient attention due to the conflict between two main control objectives in DC microgrids, i.e., voltage regulation and current sharing. By revealing a necessary and sufficient condition for achieving these two objectives, this paper proposes a novel consensus-based current sharing control law that can achieve the compromised control objective, balancing both current sharing and voltage deviation restriction. Additionally, we examine the effectiveness of the proposed control scheme for DC Microgrids that include both critical nodes and ordinary nodes, where there is a simultaneous requirement for voltage deviation limits on critical nodes and accurate current sharing among ordinary nodes. Theoretical results are verified by simulations, and the effectiveness in handling plug-and-play operations of distributed generators is also illustrated.

Key words: compromised control; current sharing; DC microgrid; Kron reduction; voltage deviation.

1 Introduction

Distributed control of DC microgrids has received extensive attention in both control and power communities (Che and Shahidehpour, 2014; De Persis et al., 2018; Dragičević et al., 2015; Liu et al., 2023). Two common objectives for DC microgrids are current sharing and voltage regulation (Dragičević et al., 2015). The former addresses the problem of sharing the total load current among distributed generators (DGs) in proportion to their current ratings, and the latter aims to regulate each bus voltage to its rated value. However, there exists a conflict between current sharing and voltage regulation (Bai et al., 2022; Han et al., 2019). Most existing control methods prioritize current sharing over voltage regulation, and can only achieve voltage balancing that regulates the steady-state average or weighted-average

voltage over all buses at a rated value (Cucuzzella et al., 2018; Liu et al., 2024; Nahata et al., 2022; Shafiee et al., 2014; Trip et al., 2019; Tucci et al., 2018).

For normal operation of loads, voltage deviations of buses from the rated value should be kept within an admissible range, e.g., 5% of the rated voltage (Nasirian et al., 2015; Prabhakaran et al., 2018). Even though accurate current sharing and voltage balancing are achieved, voltage deviations exceeding admissible ranges may cause abnormal operation or damage to certain loads. Thus, bus voltage deviations should be strictly restricted, especially for voltage-sensitive loads.

The issue of voltage deviation restriction was concerned in Han et al. (2019), and a compromised control method was proposed to achieve a trade-off between current sharing and voltage regulation. Ding et al. (2018) proposed a distributed optimal control strategy to achieve a compromised objective between accurate current sharing and voltage regulation. In Cucuzzella et al. (2018), a manifold was designed to take both current sharing and voltage regulation into consideration, in which voltage deviation can be regulated. Yet, in these studies, the mechanism of interaction between current sharing and voltage regulation is not disclosed, and thus it is hard to quantitatively adjust the accuracy of current sharing and voltage deviation regulation. Voltage deviation regula-

* This work was supported by Shenzhen Science and Technology Program under grants GXWD20231129102406001 and JCYJ20220818102416036, the Key Scientific Research Projects of Higher Education Institutions in Henan Province under grant 24A120011, and the National Natural Science Foundation of China under grant 62303133.

* Corresponding author.

Email addresses: baihandong@yrcti.edu.cn (Handong Bai), lipeng2020@hit.edu.cn (Peng Li), hwzhang@hit.edu.cn (Hongwei Zhang).

tion was further investigated in (Bai et al., 2022), where a distributed compromised controller was proposed to achieve a trade-off between accurate current sharing and reference voltage consensus. However, it cannot regulate each bus voltage to its rated value simultaneously, and thus fails when strict voltage deviation is required.

Furthermore, in the existing literature on distributed control of DC microgrids, most works treat all nodes equally. However, different types of loads have various tolerance to voltage deviations. For example, data centers are voltage-sensitive loads that often require a very strict voltage deviation of less than 2% of the rated voltage (Pratt et al., 2007), while voltage-insensitive loads like residential facilities can even tolerate a voltage deviation of 8% of the rated voltage. Therefore, in DC microgrids, nodes should be classified regarding voltage deviation and current sharing. To the best of our knowledge, such control issues have not been investigated so far. Therefore, this paper aims to investigate DC microgrids consisting of critical nodes (i.e., voltage-sensitive nodes) and ordinary nodes (i.e., voltage-insensitive ones), and design distributed control laws that can simultaneously strictly restrict voltage deviations for critical nodes and achieve accurate current sharing for ordinary nodes. The main contributions of this paper are as follows:

- Control objectives of accurate current sharing, accurate voltage consensus, and voltage-current compromise are uniformly characterized by voltage and current deviation ratios, facilitating the controller design. In addition, necessary and sufficient condition for the existence of the conflict between accurate current sharing and voltage consensus is derived.
- Kron reduction is applied to reduce the topology of the communication network for the first time. This allows us to control DC microgrids with two classes of nodes, achieving distinct control objectives.
- A generalized consensus control framework is proposed, and voltage deviation restriction of critical nodes and accurate current sharing of ordinary nodes are achieved simultaneously. The monotonicity of voltage and current deviation ratios is guaranteed, which is of practical significance for designing the trade-off factor.

2 Preliminaries and problem formulation

2.1 Notations

The identity matrix is denoted by \mathbf{E} . A zero vector or matrix with appropriate dimensions is denoted by $\mathbf{0}$. Let $\mathbf{1}_n = [1, \dots, 1]^T \in \mathbb{R}^n$. A diagonal matrix with g_i being the i -th diagonal entry is $\text{diag}(g_1, g_2, \dots, g_n)$. A matrix $\mathbf{A} = [a_{ij}] \in \mathbb{R}^{n \times n}$ is nonnegative (positive), denoted by $\mathbf{A} \geq \mathbf{0}$ ($\mathbf{A} > \mathbf{0}$), if $a_{ij} \geq 0$ ($a_{ij} > 0$), $\forall i, j$. Matrix $|\mathbf{A}|$ is the element-wise absolute value of \mathbf{A} .

2.2 Graph theory

The communication network of a DC microgrid is modeled as a graph $\mathcal{G} = (\mathcal{V}, \mathcal{E})$, where $\mathcal{V} = \{v_1, \dots, v_N\}$ de-

notes the set of nodes, i.e., DGs or buses, and $\mathcal{E} \subseteq \mathcal{V} \times \mathcal{V}$ denotes the set of edges, i.e., communication links. The adjacency matrix of a graph is $\mathcal{A} = [a_{ij}] \in \mathbb{R}^{N \times N}$, where a_{ij} is the weight of edge (v_j, v_i) , and $a_{ij} > 0$ if $(v_j, v_i) \in \mathcal{E}$; otherwise $a_{ij} = 0$. The neighbor set of node i is $\mathcal{N}_i = \{j | (v_j, v_i) \in \mathcal{E}\}$. The Laplacian matrix $\mathcal{L} = [l_{ij}] \in \mathbb{R}^{N \times N}$ of \mathcal{G} is defined as $l_{ii} = \sum_{j=1}^N a_{ij}$ and $l_{ij} = -a_{ij}$ if $i \neq j$. In this paper, \mathcal{G} is undirected and connected (Lewis et al., 2014).

2.3 DC microgrid modeling

Consider a DC microgrid consisting of N ($N > 1$) nodes and M power lines, whose electrical network has been reduced by Kron reduction (Dörfler and Bullo, 2013). A

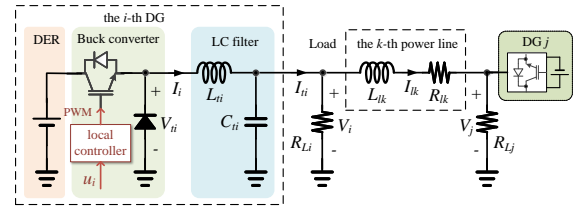


Fig. 1. Electrical scheme of the i -th DG (Trip et al., 2019)

general electrical scheme of the i -th DG is shown in Fig. 1, where V_{t_i} denotes the output voltage of the Buck converter of the i -th DG, L_{t_i} and C_{t_i} denote the inductance and capacitance of the LC filter respectively. Following standard practices (Nahata et al., 2020; Schiffer et al., 2016), we have $V_{t_i} = u_i$, where V_{t_i} is the output voltage of the i -th DG converter, and u_i is the associated control signal for this converter. Let $\mathbf{V}_t = [V_{t_1}, \dots, V_{t_N}]^T$ and $\mathbf{u} = [u_1, \dots, u_N]^T$. Then

$$\mathbf{V}_t = \mathbf{u}. \quad (1)$$

The dynamics of power lines can be modeled as

$$\mathbf{L}_l \dot{\mathbf{I}}_l = \mathbf{B}^T \mathbf{V} - \mathbf{R}_l \mathbf{I}_l, \quad (2)$$

where $\mathbf{V} = [V_1, \dots, V_N]^T$ and $\mathbf{I}_l = [I_{l_1}, \dots, I_{l_M}]^T$ denote bus voltages and the currents of power lines, respectively; $\mathbf{L}_l = \text{diag}(L_{l_1}, \dots, L_{l_M})$ and $\mathbf{R}_l = \text{diag}(R_{l_1}, \dots, R_{l_M})$ denote inductances and resistances of power lines, respectively; $\mathbf{B} = [B_{ik}] \in \mathbb{R}^{N \times M}$ denotes the incidence matrix of electrical topology of the DC microgrid, in which $B_{ik} = +1$ (-1) if the i -th bus is the source (sink) of the k -th power line; otherwise, $B_{ik} = 0$.

This paper considers loads of constant impedances with admittances $\mathbf{Y}_L = \text{diag}(Y_{L_1}, \dots, Y_{L_N})$, where $Y_{L_i} = \frac{1}{R_{L_i}}$, and Y_{L_i}, R_{L_i} are conductance and resistance of the i -th load, respectively. According to Kirchhoff's voltage and current laws, the dynamics of the output LC filters

of the converters can be modeled as

$$\mathbf{L}_t \dot{\mathbf{I}} = \mathbf{V}_t - \mathbf{V} \quad (3a)$$

$$\mathbf{C}_t \dot{\mathbf{V}} = \mathbf{I} - \mathbf{Y}_L \mathbf{V} - \mathbf{B} \mathbf{I}_l, \quad (3b)$$

where $\mathbf{I} = [I_1, \dots, I_N]^T$ denotes the output currents of the DG converters; $\mathbf{L}_t = \text{diag}(L_{t_1}, \dots, L_{t_N})$ and $\mathbf{C}_t = \text{diag}(C_{t_1}, \dots, C_{t_N})$ denote inductances and capacitances of the LC filters, respectively.

2.4 Conflict of voltage consensus and current sharing

The objectives of proportional current sharing among DGs and maintaining all bus voltages at the rated value cannot be achieved simultaneously (Liu et al., 2023). This conflict will be rigorously analyzed in the sequel. The following definitions and fact are instrumental.

Definition 1 (Bai et al., 2022) In a DC microgrid, the voltage deviation ratio and the current deviation ratio for the i -th DG are defined respectively as

$$\Delta_i^V = \frac{V_i - V_{rat}}{V_{rat}} \quad \text{and} \quad \Delta_i^I = \frac{I_i^{pu} - I_{avg}^{pu}}{I_{avg}^{pu}},$$

where V_{rat} is the rated bus voltage of the DC microgrid, $I_i^{pu} = I_i/I_i^*$ is the output per-unit current of the DG at node i with $I_i^* > 0$ being the current capacity of the i -th DG, and $I_{avg}^{pu} = \sum_{i=1}^N I_i^{pu}/N$. Furthermore, define the maximum voltage deviation ratio and the maximum current deviation ratio of the DC microgrid as $\Delta_{max}^V = \|\Delta^V\|_\infty$ and $\Delta_{max}^I = \|\Delta^I\|_\infty$, respectively, where $\Delta^V = [\Delta_1^V, \dots, \Delta_N^V]^T$, $\Delta^I = [\Delta_1^I, \dots, \Delta_N^I]^T$.

Based on the above notions, accurate current sharing and voltage consensus are further defined.

Definition 2 (Accurate current sharing) In a DC microgrid, accurate current sharing among DGs is achieved if $\Delta_{max}^I = 0$, i.e., $\frac{I_i}{I_i^*} = \dots = \frac{I_N}{I_N^*}$.

Definition 3 (Accurate voltage consensus) In a DC microgrid, accurate voltage consensus among buses is achieved if $\Delta_{max}^V = 0$, i.e., $V_i = \dots = V_N = V_{rat}$.

The following Fact shows when these two objectives conflict with each other.

Fact 1 Consider a DC microgrid described by (1), (2) and (3). In steady state, accurate current sharing and accurate voltage consensus can be achieved simultaneously if and only if $Y_{L_i} > 0$ for all $i \in \{1, 2, \dots, N\}$ and

$$\frac{I_1^*}{Y_{L_1}} = \frac{I_2^*}{Y_{L_2}} = \dots = \frac{I_N^*}{Y_{L_N}}. \quad (4)$$

Remark 1 Equation (4) implies that the rated output current of each node matches its load. For this case, when the DG of each node injects its rated current, i.e., $I_i = I_i^*$, the steady state bus voltages $V_i = I_i/Y_{L_i} = I_i R_{L_i}$ of all nodes are equal. Then there is no voltage difference

between buses and no current flows between them.

When (4) does not hold, a conflict emerges and a concept of voltage-current compromise is introduced.

Definition 4 (Voltage-current compromise) Let $\bar{\Delta}^V$ be the maximum voltage deviation ratio when accurate current sharing is achieved, and $\bar{\Delta}^I$ be the maximum current deviation ratio when accurate voltage consensus is achieved. Then, voltage-current compromise is established if $\Delta_{max}^V < \bar{\Delta}^V$ and $\Delta_{max}^I < \bar{\Delta}^I$.

2.5 Problem formulation

A practical DC microgrid usually consists of two classes of loads, i.e., voltage-sensitive and voltage-insensitive loads. While it is necessary to restrict bus voltage deviations for voltage-sensitive loads within their normal operational ranges, voltage regulation of voltage-insensitive loads is not a major concern. Thus, we shall call voltage-sensitive nodes as *critical nodes* and voltage-insensitive nodes as *ordinary nodes*.

Consider a DC microgrid with N nodes and let $\mathcal{M} = \{1, \dots, N\}$. Without loss of generality, let $\mathcal{M}_c = \{1, \dots, m\}$ be the set of critical nodes, and $\mathcal{M}_o = \{m+1, \dots, N\}$ be the set of ordinary nodes. The main problem can then be formulated as follows.

Problem 1 Consider a DC microgrid described by (1), (2) and (3), which consists of m critical nodes and $N-m$ ordinary nodes. Let $\Gamma_V \in [0, \bar{\Delta}_c^V]$ be a user defined voltage deviation index, where $\bar{\Delta}_c^V$ is the maximum voltage deviation ratio of critical nodes when their accurate current sharing is achieved. Let V_{rat} be the desired rated value for critical nodes. Design a distributed controller in the form $u_i(\theta, \omega, I_i, V_i, \phi_j | j \in \mathcal{N}_i)$, where θ and ω are design parameters and ϕ_j stands for some neighborhood variables, such that the following objectives can be obtained.

(a) For critical nodes, their maximum voltage deviation ratio is restricted by Γ_V and their average voltage is regulated to the rated value, i.e.,

$$\max_{i \in \mathcal{M}_c} \Delta_i^V \leq \Gamma_V, \quad \frac{1}{m} \sum_i^m V_i = V_{rat}, \quad i \in \mathcal{M}_c \quad (5)$$

(b) For critical nodes, their voltage deviation ratios Δ_i^V can be monotonically adjusted by θ .

(c) For ordinary nodes, accurate current sharing is achieved and the per-unit current $I_i^{pu} = I_i/I_i^*$ can be monotonically adjusted by the design parameter ω , i.e., $I_i/I_i^* = I_j/I_j^* = \alpha(\omega)$, $\forall i, j \in \mathcal{M}_o$, where the function $0 \leq \alpha(\omega) \leq 1$ is a monotonic function of ω .

Remark 2 Problem 1 focuses on the case where $\Gamma_V \in [0, \bar{\Delta}_c^V]$. Smaller Γ_V implies more strict voltage deviation at critical nodes. For the extreme case of $\Gamma_V = 0$, voltages of all critical nodes should achieve consensus. The ability to monotonically adjust $\Delta_i^V, i \in \mathcal{M}_c$ along a single parameter θ is practically important, as it provides practitioners a convenient way to adjust the voltage deviation of critical nodes. For a very conservative value $\Gamma_V > \bar{\Delta}_c^V$, one only needs to control all critical nodes

to achieve accurate current sharing, and then the Objective (a) will be automatically achieved. In this case, no voltage-current compromise is necessary and many existing works can deal with it. The Objective (c) implies that the portion of contribution of ordinary nodes to the microgrid can be monotonically tuned by the parameter ω .

3 Compromised controller design

3.1 Average voltage estimation for critical nodes

To address Problem 1, we first design an average voltage estimator of critical nodes. Inspired by the average consensus algorithm proposed in Kia et al. (2019), an average voltage observer for microgrid can be put as

$$\begin{bmatrix} \dot{\bar{\mathbf{V}}}_c \\ \dot{\bar{\mathbf{V}}}_o \end{bmatrix} = \begin{bmatrix} \dot{\mathbf{V}}_c \\ \dot{\mathbf{V}}_o \end{bmatrix} - \begin{bmatrix} \mathcal{L}_{11} & \mathcal{L}_{12} \\ \mathcal{L}_{21} & \mathcal{L}_{22} \end{bmatrix} \begin{bmatrix} \bar{\mathbf{V}}_c \\ \bar{\mathbf{V}}_o \end{bmatrix}, \quad (6)$$

where $\bar{\mathbf{V}}_c$ and \mathbf{V}_c are the average voltage estimates and measured voltages of all critical nodes, and $\bar{\mathbf{V}}_o$ and \mathbf{V}_o are the average voltage estimates and measured voltages of all ordinary nodes. Manipulating (6) yields that $\dot{\bar{\mathbf{V}}}_c = \dot{\mathbf{V}}_c - \mathcal{L}_{22}[\mathcal{L}\bar{\mathbf{V}}_c + \mathcal{L}_{12}\mathcal{L}_{22}^{-1}(\dot{\mathbf{V}}_o - \dot{\mathbf{V}}_o)]$, with $\mathcal{L}_{22}[\mathcal{L} = \mathcal{L}_{11} - \mathcal{L}_{12}\mathcal{L}_{22}^{-1}\mathcal{L}_{21}$. Obviously, if $\dot{\mathbf{V}}_o - \dot{\mathbf{V}}_o = \mathbf{0}$, we have $\dot{\bar{\mathbf{V}}}_c = \dot{\mathbf{V}}_c - \mathcal{L}_{22}[\mathcal{L}\bar{\mathbf{V}}_c$. Accordingly, we design an estimator $\dot{\tilde{\mathbf{V}}}_i$ of average voltage among critical nodes as

$$\dot{\tilde{\mathbf{V}}}_i = \dot{\mathbf{V}}_i + \sum_{j=1}^N a_{ij} (\tilde{\mathbf{V}}_j - \tilde{\mathbf{V}}_i), \quad \forall i \in \mathcal{M}_c \quad (7)$$

$$\tilde{\mathbf{V}}_k = \frac{\sum_{j=1}^N a_{kj} \tilde{\mathbf{V}}_j}{\sum_{j=1}^N a_{kj}}, \quad \forall k \in \mathcal{M}_o \quad (8)$$

where a_{ij}, a_{kj} are the elements of the adjacency matrix \mathcal{A} of the communication graph.

The above procedure shows how to eliminate ordinary nodes from the communication graph using Kron reduction technique (Caliskan and Tabuada, 2014; Dörfler et al., 2018). This is crucial because it decouples two classes of nodes in a microgrid, thereby simplifying the controller design to meet various objectives.

Proposition 1 Consider the DC microgrid (1), (2) and (3) consisting of critical nodes $i \in \mathcal{M}_c$ and ordinary nodes $k \in \mathcal{M}_o$. In steady state, the estimation governed by (7) and (8) converges to the average voltage among the critical nodes, i.e., $\lim_{t \rightarrow \infty} \tilde{\mathbf{V}}_i = \frac{1}{m} \sum_{j=1}^m \mathbf{V}_j$, $\forall i \in \mathcal{M}$.

3.2 Distributed control law design

A distributed secondary control law has been broadly used for accurate current sharing with a generic form:

$$\dot{x}_i = \sum_{j=1}^N a_{ij} \left(\frac{I_j}{I_j^*} - \frac{I_i}{I_i^*} \right), \quad \forall i \in \mathcal{M}, \quad (9)$$

where x_i denotes different notions in different works, such as voltage correction term in Nasirian et al. (2015), additional state variable in Nahata et al. (2022) and voltage deviation between voltage reference and node voltage in Tucci et al. (2018). In steady state, accurate current sharing is achieved. However, the distinct objectives for critical and ordinary nodes, as addressed in Problem 1, have not been simultaneously considered in all aforementioned works. Inspired by (9), we shall propose a general consensus-based control framework that can simultaneously address separate objectives of Problem 1.

Before designing the compromised control laws for critical nodes, we need the following preliminary result. Let

$$\mathbf{Y} = \mathbf{B}\mathbf{R}_l^{-1}\mathbf{B}^T \text{ and } \bar{\mathbf{Y}} = \mathbf{Y} + \mathbf{Y}_L = \begin{bmatrix} \bar{\mathbf{Y}}_{11} & \mathbf{Y}_{12} \\ \mathbf{Y}_{21} & \bar{\mathbf{Y}}_{22} \end{bmatrix}, \text{ where } \bar{\mathbf{Y}}_{11} \in \mathbb{R}^{m \times m}, \mathbf{Y}_{12} \in \mathbb{R}^{m \times (N-m)}, \mathbf{Y}_{21} \in \mathbb{R}^{(N-m) \times m}, \bar{\mathbf{Y}}_{22} \in \mathbb{R}^{(N-m) \times (N-m)}.$$

Lemma 1 Consider the DC microgrid (1), (2) and (3) consisting of critical nodes $i \in \mathcal{M}_c$ and ordinary nodes $k \in \mathcal{M}_o$. In steady state, voltage consensus of critical nodes can be achieved, i.e., $\bar{\mathbf{V}}_i = V_{rat}$, $\forall i \in \mathcal{M}_c$, if and only if $\mathbf{I}_c - \mathbf{Y}_{12}\bar{\mathbf{Y}}_{22}^{-1}\mathbf{I}_o = V_{rat}\bar{\mathbf{Y}}_{22}|\mathbf{Y}\mathbf{1}_m$, where $\mathbf{I}_c = [I_1, \dots, I_m]^T$, $\bar{\mathbf{Y}}_{22}|\bar{\mathbf{Y}} = \bar{\mathbf{Y}}_{11} - \mathbf{Y}_{12}\bar{\mathbf{Y}}_{22}^{-1}\mathbf{Y}_{21}$ is Schur complement of $\bar{\mathbf{Y}}_{22}$ with respect to $\bar{\mathbf{Y}}$.

Lemma 1 establishes a basis for achieving voltage consensus in critical nodes. To enable voltage-current compromise, inspired by (9), a trade-off factor is incorporated into the generalized consensus control protocol

$$\dot{x}_i = \sum_{j=1}^N a_{ij} \left(\frac{I_j}{I_{r_j}} - \frac{I_i}{I_{r_i}} \right), \quad \forall i \in \mathcal{M}, \quad (10)$$

with

$$I_{r_k} = \begin{cases} \theta I_k^* + (1 - \theta) I_{b_k}, & \forall k \in \mathcal{M}_c, \\ I_k^*, & \forall k \in \mathcal{M}_o, \end{cases} \quad (11a)$$

$$\mathbf{I}_{b_c} = [I_{b_1}, \dots, I_{b_m}]^T = \omega V_{rat} \bar{\mathbf{Y}}_{22}|\bar{\mathbf{Y}}\mathbf{1}_m + \mathbf{Y}_{12}\bar{\mathbf{Y}}_{22}^{-1}\mathbf{I}_o^*, \quad (11b)$$

where $\theta \in [0, 1]$ is a trade-off factor indicating the compromised degree; $\mathbf{I}_o^* = [I_{m+1}^*, \dots, I_N^*]^T$ is the rated current vector of ordinary nodes; ω is a design parameter for adjusting the output currents of ordinary nodes. The tuning rules of θ and ω are provided in Proposition 2.

Remark 3 Note that (10) is generally a part of the con-

trol law u_i . For control schemes incorporating (9) (e.g., Liu et al. (2024); Nahata et al. (2022); Nasirian et al. (2015); Tucci et al. (2018)), replacing the constant I_i^* in (9) with the adjustable I_{r_i} in (11a) can upgrade the performance of the control schemes from accurate current sharing to a voltage-current compromise. Generally, this performance improvement does not affect the stability analysis of the closed-loop system, and thus is omitted.

Let droop control serve as the primary control of the DC microgrid, receiving the compensation signal x_i from the secondary control (10). Additionally, an integral signal y_i is adopted to regulate the average voltage to the rated value. Then the distributed controller u_i is proposed as

$$u_i = V_{rat} - r_i I_i + x_i + y_i, \forall i \in \mathcal{M}, \quad (12)$$

$$\dot{y}_i = V_{rat} - \tilde{V}_i, \quad (13)$$

where r_i is the droop coefficient.

3.3 Steady state analysis

Theorem 1 Consider the DC microgrid (1), (2) and (3) consisting of the critical nodes $i \in \mathcal{M}_c$ and the ordinary nodes $k \in \mathcal{M}_o$. These two classes of nodes are governed by (7), (8), (10), (11), (12), and (13). Then, the following statements hold for steady state:

- (a) Average voltage regulation among critical nodes is achieved, i.e., $\frac{1}{m} \sum_{j=1}^m V_j = V_{rat}$.
- (b) For a given θ , the output currents of DGs satisfy

$$\frac{I_i}{I_{r_i}} = \frac{I_k}{I_k^*} = \frac{1}{\mu\theta + \omega(1-\theta)}, \forall i \in \mathcal{M}_c, k \in \mathcal{M}_o \quad (14)$$

where $\mu = \frac{1}{mV_{rat}} \mathbb{1}_m^T (\bar{\mathbf{Y}}_{22} | \bar{\mathbf{Y}})^{-1} (\mathbf{I}_c^* - \mathbf{Y}_{12} \bar{\mathbf{Y}}_{22}^{-1} \mathbf{I}_o^*)$ with $\mathbf{I}_c^* = [I_1^*, \dots, I_m^*]^T$ being the rated current vector of critical nodes.

- (c) Let $\Delta_c^V(\theta)$ and $\Delta_c^I(\theta)$ denote the voltage and current deviation ratio of critical nodes, respectively. Then, $|\Delta_c^V(\theta)|$ and $|\Delta_c^I(\theta)|$ are monotonically increasing and decreasing, respectively, on $\theta \in [0, 1]$, and

$$\Delta_c^V(\theta) = \frac{\theta}{(\mu - \omega)\theta + \omega} \Psi_1 \quad (15a)$$

$$\Delta_c^I(\theta) = \frac{1 - \theta}{\theta(1/\bar{I}_{b_c}^{pu} - 1) + 1} \Delta_{b_c}^I, \quad (15b)$$

where $\Psi_1 = \frac{1}{V_{rat}} (\bar{\mathbf{Y}}_{22} | \bar{\mathbf{Y}})^{-1} (\mathbf{I}_c^* - \mathbf{Y}_{12} \bar{\mathbf{Y}}_{22}^{-1} \mathbf{I}_o^*) - \mu \mathbb{1}_m$, $\bar{I}_{b_c}^{pu} = \frac{1}{m} \mathbb{1}_m^T \mathbf{I}_{b_c}^{pu}$ and $\Delta_{b_c}^I = (\mathbf{I}_{b_c}^{pu} - \bar{I}_{b_c}^{pu} \mathbb{1}_m) / \bar{I}_{b_c}^{pu}$ with $\mathbf{I}_{b_c}^{pu} = \text{diag}(\mathbf{I}_c^*)^{-1} \mathbf{I}_{b_c}$. Particularly, for $\theta \in [0, 1]$, we have

$$\begin{cases} \min_{\theta} |\Delta_c^V(\theta)| = \Delta_c^V(0) = 0 \\ \max_{\theta} |\Delta_c^V(\theta)| = |\Delta_c^V(1)| = \frac{1}{\mu} |\Psi_1|, \end{cases} \quad (16)$$

$$\begin{cases} \min_{\theta} |\Delta_c^I(\theta)| = \Delta_c^I(1) = 0 \\ \max_{\theta} |\Delta_c^I(\theta)| = |\Delta_c^I(0)| = |\Delta_{b_c}^I|. \end{cases}$$

- (d) Voltage $\mathbf{V}_o = [V_{m+1}, \dots, V_N]$ of ordinary nodes is

$$\mathbf{V}_o = \frac{1}{\theta(\mu - \omega) + \omega} \left(\Omega_2 - \frac{\omega}{\mu - \omega} \Omega_1 \right) + \frac{1}{\mu - \omega} \Omega_1,$$

where $\Omega_1 = -(\bar{\mathbf{Y}}_{11} | \bar{\mathbf{Y}})^{-1} \mathbf{Y}_{21} \bar{\mathbf{Y}}_{11}^{-1} (\mathbf{I}_c^* - \mathbf{I}_{b_c})$ and $\Omega_2 = (\bar{\mathbf{Y}}_{11} | \bar{\mathbf{Y}})^{-1} (\mathbf{I}_o^* - \mathbf{Y}_{21} \bar{\mathbf{Y}}_{11}^{-1} \mathbf{I}_{b_c})$. Each entry of \mathbf{V}_o is a monotone function on $\theta \in [0, 1]$.

This result shows that the degree of voltage-current compromise of critical nodes can be adjusted by tuning θ . The monotonicity of $|\Delta_c^V(\theta)|$ guarantees that strict voltage deviation at critical nodes can be achieved.

Remark 4 Theorem 1 implies that accurate current sharing of ordinary nodes can always be achieved for any θ , while critical nodes can only achieve accurate current sharing when $\theta = 1$; in addition, critical nodes achieve voltage consensus when $\theta = 0$ and a voltage-current compromise when $\theta \in (0, 1)$.

3.4 Voltage deviation restriction for critical nodes

The following proposition provides guidelines for designing θ and ω based on a given Γ_V .

Proposition 2 Consider a DC microgrid with the same conditions as those in Theorem 1. The following statements hold.

- (a) Given a positive Γ_V , voltage deviation restriction for the critical nodes is achieved when $\theta \in [0, \theta_d]$, where θ_d is designed as

$$\theta_d = \begin{cases} 1, & \text{when } \|\Delta_c^V(1)\|_{\infty} < \Gamma_V \\ \frac{\omega \Gamma_V / (\mu - \omega)}{\|\Psi_1\|_{\infty} - \Gamma_V}, & \text{when } 0 < \Gamma_V \leq \|\Delta_c^V(1)\|_{\infty} \\ 0, & \text{when } \Gamma_V = 0. \end{cases}$$

- (b) Given $\theta \in [0, 1]$, the adjustable range of ω is

$$\mathcal{W} = \left[\max_i \left\{ \frac{\zeta_i}{\nu_i} \right\}, +\infty \right), i \in \mathcal{M}_c, \forall \nu_i > 0,$$

where $[\zeta_1, \dots, \zeta_m]^T = \frac{-\theta}{1-\theta} \mathbf{I}_c^* - \mathbf{Y}_{12} \bar{\mathbf{Y}}_{22}^{-1} \mathbf{I}_o^*$, and $[\nu_1, \dots, \nu_m]^T = V_{rat} \bar{\mathbf{Y}}_{22} | \bar{\mathbf{Y}} \mathbb{1}_m$.

- (c) The output per-unit currents of DGs at the ordinary nodes \mathbf{I}_o^{pu} are monotonically decreasing on $\omega \in \mathcal{W}$.
- (d) The sum of the output currents of DGs at the critical nodes $\mathbb{1}_m^T \mathbf{I}_c$ is monotonically increasing on $\omega \in \mathcal{W}$ if $\theta \mathbb{1}_m^T \mathbf{I}_c^* + (1 - \theta) \mathbb{1}_m^T \mathbf{Y}_{12} \bar{\mathbf{Y}}_{22}^{-1} \mathbf{I}_o^* < 0$.

Remark 5 According to Theorem 1 and Propositions 1 and 2, Problem 1 can be addressed by the control scheme (7), (8), (10), (11) and (12), (13). Specifically, (14) in Theorem 1 and Statement (b) in Proposition 2 show that

Objective (c) is achieved; Statement (a) in Theorem 1 and Statement (a) in Proposition 2 jointly ensure Objective (a); Statement (c) in Theorem 1 illustrates the achievement of Objective (b).

4 Simulation examples

Consider a DC microgrid composed of 7 DGs, as shown in Fig. 2. Without loss of generality, let the weight of each communication link be $a_{ij} = 20$, where a greater a_{ij} is beneficial to faster convergence without changing the steady-state value (Lewis et al., 2014).

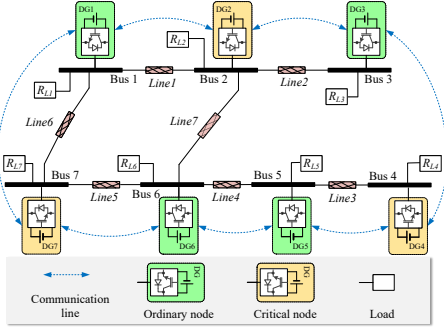


Fig. 2. DC microgrid with critical nodes $\{2,4,7\}$ and ordinary nodes $\{1,3,5,6\}$

The rated voltage of the microgrid is set to $V_{rat} = 380V$. Let $\mathbf{I}^* = \text{diag}(30, 30, 20, 20, 40, 40, 40)$ A, $\mathbf{L}_t = \text{diag}(2, 2.2, 1.8, 2.5, 3, 2.6, 2.3)$ mH, $\mathbf{C}_t = \text{diag}(3, 2.5, 2.8, 2.5, 2.3, 3, 2.6)$ mF, $\mathbf{R}_L = \text{diag}(50, 20, 26, 35, 38, 23, 40)$ Ω . The parameters of power lines are $R_{l_1} = 2\Omega$, $L_{l_1} = 20\mu\text{H}$; $R_{l_2} = 2.4\Omega$, $L_{l_2} = 25\mu\text{H}$; $R_{l_3} = 2\Omega$, $L_{l_3} = 20\mu\text{H}$; $R_{l_4} = 4\Omega$, $L_{l_4} = 35\mu\text{H}$; $R_{l_5} = 2\Omega$, $L_{l_5} = 20\mu\text{H}$; $R_{l_6} = 2\Omega$, $L_{l_6} = 20\mu\text{H}$; $R_{l_7} = 2\Omega$, $L_{l_7} = 20\mu\text{H}$.

The simulation examples consist of two cases, where the control laws (7), (8), (10), (11), (12), and (13) are used.

Case I: Compromised control for critical nodes

For critical nodes, the objective is to restrict the voltage deviation within $[0, \Gamma_V]$, where $\Gamma_V = 2\%$, meanwhile maintaining the current sharing performance of ordinary nodes. The following results show how θ and ω affect the system performance.

During $t \in [0, 5)s$, let $\theta = 1$, $\omega = 2$ in controller (11). In steady state, Fig. 3(b) shows current sharing for all nodes is achieved, while Fig. 3(a) shows the voltage deviation of node 7 is beyond the admissible range (shaded area).

During $t \in [5, 10)s$, we set $\theta = 0.63$ and $\omega = 2$. In fact, according to Theorem 1 and Proposition 2, the Δ_{max}^V of critical nodes can be restricted within $[0, 0.02]$ by setting $\theta \in [0, 0.63]$ when $\omega = 2$, which is shown in Fig. 3(a). At the same time, the current sharing performance of critical nodes is degraded, which shows a compromise between voltage consensus and current sharing of critical nodes. It is noted from Fig. 3(b) that the current sharing of ordinary nodes is still maintained.

During $t \in [10, 15)s$, we set $\theta = 0$ and $\omega = 2$. Voltage consensus of all critical nodes is achieved and $\lim_{t \rightarrow \infty} V_i(t) = V_{rat}, \forall i \in \mathcal{M}_c$ (see Fig. 3(a)). In this case, the critical nodes have the worst current sharing performance (see Fig. 3(b)). At the same time, the current sharing is still achieved for ordinary nodes.

During $t \in [15, 20)s$, we keep $\theta = 0$ and tune ω from 2 to 1.71. It is observed that the output currents of ordinary nodes increase (see Fig. 3(b)). Meanwhile, the output currents of critical nodes decrease accordingly. Also note that when $\omega = 1.71$, $I_7^{pu} = 0$, the per-unit currents of ordinary nodes reach the admissible maximum $I_i^{pu} = 0.585, i = \{1, 3, 5, 6\}$ (see Fig. 3(b)). In this phase, since $\theta = 0$, the voltage consensus for critical nodes still holds, i.e., $\lim_{t \rightarrow \infty} V_i(t) = V_{rat}, \forall i \in \mathcal{M}_c$ (see Fig. 3(a)).

Moreover, we can see that the average voltage of critical nodes can always be regulated to the rated value of 380V (see Fig. 3(a)), and current sharing for ordinary nodes can also be achieved (see Fig. 3(b)), both independent of the choices of θ and ω .

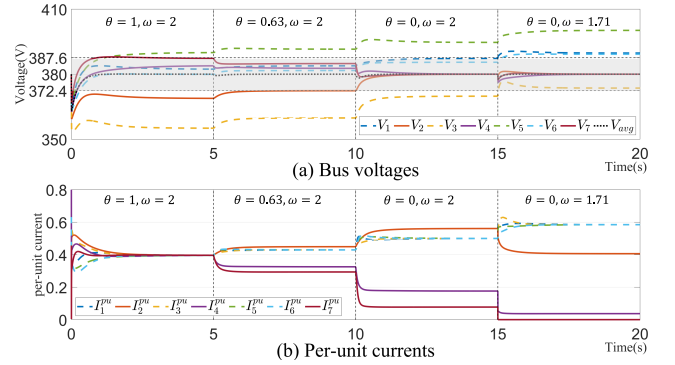


Fig. 3. Simulation results of Case I. The shaded area corresponds to the admissible voltage range for critical nodes.

Case II: Plug-and-play (PnP) operation of DGs

The configurations of critical nodes and ordinary nodes are the same as in Case I. Let $\theta = 0$ and $\omega = 2$. This setting corresponds to accurate voltage consensus of critical nodes and accurate current sharing of ordinary nodes. To illustrate the performance of the proposed control laws under the PnP of DGs connected to ordinary node and critical node respectively, we perform two simulations.

(a) PnP of DG at ordinary node

During $t \in [0, 4)s$, all nodes are normally operated. Figure 4(a) shows that all critical node voltages are regulated to 380V, i.e., accurate voltage consensus is achieved, while currents are accurately shared among all ordinary nodes (i.e., 1, 3, 5, 6) (see Fig. 4(b)).

During $t \in [4, 12)s$, the DG of node 6 is plugged out from the DC microgrid. Then the output current of DG 6 becomes zero immediately at $t = 4s$ (see Fig. 4(b)), and meanwhile, the bus voltage of node 6 is dropped from 385.5V to 369V (see Fig. 4(a)). However, voltage consensus of critical nodes and accurate current sharing

of the rest ordinary nodes are still achieved at steady state.

During $t \in [12, 20]s$, the DG of node 6 is plugged back into the DC microgrid. It can be observed from Fig. 4 that bus voltages and per-unit currents of all nodes are successfully restored.

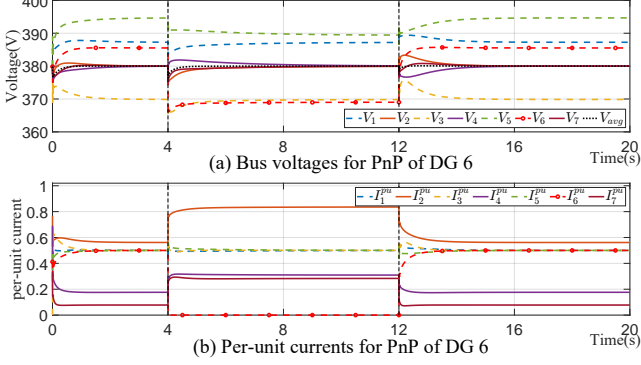


Fig. 4. Simulation results for Case II (a): 4(a) and 4(b) depict the PnP process of node 6, an ordinary node. At $t = 4s$, the DG of nodes 6 is unplugged, and at $t = 12s$, it is plugged back into the microgrid.

(b) PnP of DG at critical node

To unplug the DG at critical node 4, the critical node must first be degraded as an ordinary node, and all other critical node controllers should be updated accordingly. Then, the DG of this node can be unplugged. Reconnecting follows the exact reverse procedure. Simulation results are shown in Fig. 5(a) and 5(b). During $t \in [4, 12]s$, the output current of DG 4 drops to zero immediately at $t = 4s$, and meanwhile, the bus voltage of node 4 is dropped continuously from 380V to 362V. However, voltage consensus of the rest of the critical nodes $\{2, 7\}$ and accurate current sharing of the ordinary nodes can still be achieved at the steady state. After $t = 12s$, both voltages and per-unit currents recover.

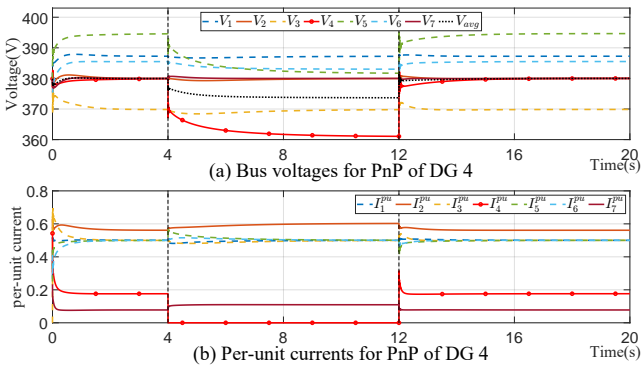


Fig. 5. Simulation results for Case II (b): 5(a) and 5(b) depict the PnP process of node 4, a critical node. At $t = 4s$, the DG of nodes 4 is unplugged, and at $t = 12s$, it is plugged back into the microgrid.

5 Conclusion

This paper proposed a voltage-current compromised control scheme for multi-bus DC microgrids. By introducing voltage deviation ratio and current deviation ratio, we formulated three objectives of accurate current sharing, voltage consensus and voltage-current compromise in a unified manner, and figured out a necessary and sufficient condition for the conflict between accurate current sharing and voltage consensus. For a class of DC microgrids consisting of critical nodes and ordinary nodes, we proposed a distributed compromised control law such that the bus voltage deviation of all critical nodes can be arbitrarily restricted without sacrificing accurate current sharing of those ordinary nodes, and the degree of compromise between voltage deviation and current sharing can be easily adjusted by a single trade-off parameter. It is worth noting that the proposed algorithm can extend various existing current sharing control methods to a compromised objective. This control algorithm also works under PnP settings.

Appendix

A Proof of Fact 1

Letting $\dot{I}_l = 0$, $\dot{I} = 0$ and $\dot{V} = 0$ in (2) and (3) and eliminating I_l yields the steady state model

$$V_t - V = 0 \quad (\text{A.1a})$$

$$I - Y_L V - YV = 0, \quad (\text{A.1b})$$

where $Y = BR_l^{-1}B^T$ is the admittance matrix of the DC microgrid, and it is an irreducible Laplacian with nonnegative eigenvalues (Dörfler et al., 2018). Then $(Y + Y_L)^{-1} > 0$ if and only if $Y_L \geq 0$ and $Y_L \neq 0$. Let $\Delta V = V - V_{rat}\mathbb{1}_N$. Then (A.1b) can be put as $I = (Y + Y_L)(V_{rat}\mathbb{1}_N + \Delta V)$. Moreover, by noticing $\Delta^V = \Delta V / V_{rat}$, we have

$$\Delta^V = (Y + Y_L)^{-1} \left(\frac{I}{V_{rat}} - Y_L \mathbb{1}_N \right). \quad (\text{A.2})$$

It implies that $\Delta^V = 0$ if and only if $I = V_{rat}Y_L\mathbb{1}_N$. Moreover, when accurate current sharing is attained, we have $I = \alpha I^*$ with α being a positive constant. Thus $\Delta^V = 0$ and $\Delta^I = 0$ if and only if $I^* = \frac{V_{rat}}{\alpha} Y_L \mathbb{1}_N$.

B Proof of Proposition 1

One can rewrite (7) and (8) in compact form as follows,

$$\begin{bmatrix} \dot{\tilde{V}}_1 \\ 0 \end{bmatrix} = \begin{bmatrix} \dot{V}_1 \\ 0 \end{bmatrix} - \begin{bmatrix} \mathcal{L}_{11} & \mathcal{L}_{12} \\ \mathcal{L}_{21} & \mathcal{L}_{22} \end{bmatrix} \begin{bmatrix} \tilde{V}_1 \\ \tilde{V}_2 \end{bmatrix}. \quad \text{Then, it holds}$$

that $\dot{\tilde{V}}_1 = \dot{V}_1 - \mathcal{L}_{22}|\mathcal{L}\tilde{V}_1$. Since the graph associated with \mathcal{L} is undirected and connected, according to Dörfler and Bullo (2013), $\mathcal{L}_{22}|\mathcal{L}$ is a symmetric Laplacian, and the graph associated with $\mathcal{L}_{22}|\mathcal{L}$ is undirected and connected. Hence, according to Kia et al. (2019), we have

$\lim_{t \rightarrow \infty} \tilde{V}_i = \frac{1}{m} \sum_{j=1}^m V_j, \forall i \in \mathcal{M}$.

C Proof of Lemma 1

The steady state equation (A.1b) can be rewritten as,

$$\begin{bmatrix} \mathbf{I}_c \\ \mathbf{I}_o \end{bmatrix} = \begin{bmatrix} \bar{\mathbf{Y}}_{11} & \mathbf{Y}_{12} \\ \mathbf{Y}_{21} & \bar{\mathbf{Y}}_{22} \end{bmatrix} \begin{bmatrix} \mathbf{V}_c \\ \mathbf{V}_o \end{bmatrix}, \quad (\text{C.1})$$

where $\mathbf{I}_c, \mathbf{V}_c \in \mathbb{R}^m$ are the steady state currents and voltages of critical nodes, respectively; and $\mathbf{I}_o, \mathbf{V}_o \in \mathbb{R}^{N-m}$ are similarly defined for ordinary nodes. A straightforward manipulation to (C.1) yields

$$\mathbf{I}_c = \bar{\mathbf{Y}}_{22} | \bar{\mathbf{Y}} \mathbf{V}_c + \mathbf{Y}_{12} \bar{\mathbf{Y}}_{22}^{-1} \mathbf{I}_o. \quad (\text{C.2})$$

Let $\Delta^{V_c} = \frac{V_c}{V_{rat}} - \mathbf{1}_m$. Then (C.2) can be put as $\mathbf{I}_c = V_{rat} \bar{\mathbf{Y}}_{22} | \bar{\mathbf{Y}} \mathbf{1}_m + V_{rat} \bar{\mathbf{Y}}_{22} | \bar{\mathbf{Y}} \Delta^{V_c} + \mathbf{Y}_{12} \bar{\mathbf{Y}}_{22}^{-1} \mathbf{I}_o$. Further, $\Delta^{V_c} = \frac{1}{V_{rat}} (\bar{\mathbf{Y}}_{22} | \bar{\mathbf{Y}})^{-1} (\mathbf{I}_c - V_{rat} \bar{\mathbf{Y}}_{22} | \bar{\mathbf{Y}} \mathbf{1}_m - \mathbf{Y}_{12} \bar{\mathbf{Y}}_{22}^{-1} \mathbf{I}_o)$. Since $\mathbf{Y}^{-1} > 0$, it holds that $(\bar{\mathbf{Y}}_{22} | \bar{\mathbf{Y}})^{-1} > 0$. Then it is clear that $\Delta^{V_c} = 0$ if and only if $\mathbf{I}_c - \mathbf{Y}_{12} \bar{\mathbf{Y}}_{22}^{-1} \mathbf{I}_o = V_{rat} \bar{\mathbf{Y}}_{22} | \bar{\mathbf{Y}} \mathbf{1}_m$.

D Proof of Theorem 1

(a) According to Proposition 1, it holds that $\tilde{V}_i = \frac{1}{m} \sum_{j=1}^m V_j$ in steady state. Considering $\dot{y}_i = 0$ in (13) (please refer to Nasirian et al. (2015) for the detailed proof), we have $\tilde{V}_i = \frac{1}{m} \sum_{j=1}^m V_j = V_{rat}$.

(b) Put (10) into compact form as $\dot{\mathbf{X}} = -\mathcal{L} \text{diag}(\mathbf{I}_r)^{-1} \mathbf{I}$. Since $\mathcal{G}(\mathcal{A})$ is undirected and connected, $\mathcal{L} \mathbf{1}_N = 0$ (Lewis et al., 2014). Therefore, since $\dot{\mathbf{X}} = 0$ in steady state, $\text{diag}(\mathbf{I}_r)^{-1} \mathbf{I} = \alpha \mathbf{1}_N$. It is straightforward to yield $\frac{I_1}{I_{r1}} = \dots = \frac{I_m}{I_{rm}} = \frac{I_{m+1}}{I_{m+1}^*} = \dots = \frac{I_N}{I_N^*} = \alpha$. Substituting $\mathbf{I}_c = \alpha \mathbf{I}_{r_c} = \alpha (\theta \mathbf{I}_c^* + (1 - \theta) \mathbf{I}_{b_c})$ and $\mathbf{I}_o = \alpha \mathbf{I}_o^*$ into (C.2) yields $\alpha (\theta (\mathbf{I}_c^* - \mathbf{I}_{b_c}) + \mathbf{I}_{b_c}) = \bar{\mathbf{Y}}_{22} | \bar{\mathbf{Y}} \mathbf{V}_c + \mathbf{Y}_{12} \bar{\mathbf{Y}}_{22}^{-1} \alpha \mathbf{I}_o^*$. In addition, voltage balancing for critical nodes implies $\mathbf{V}_c = V_{rat} (\mathbf{1}_m + \Delta_c^V)$ with $\mathbf{1}_m^T \Delta_c^V = 0$. Consequently,

$$\begin{aligned} \alpha (\bar{\mathbf{Y}}_{22} | \bar{\mathbf{Y}})^{-1} (\theta (\mathbf{I}_c^* - \mathbf{I}_{b_c}) + \omega V_{rat} \bar{\mathbf{Y}}_{22} | \bar{\mathbf{Y}} \mathbf{1}_m) \\ = V_{rat} (\mathbf{1}_m + \Delta_c^V). \end{aligned} \quad (\text{D.1})$$

Pre-multiplying both sides of (D.1) by $\mathbf{1}_m^T$ gives $\alpha = \frac{1}{\theta \mu + \omega (1 - \theta)}$. Since $\omega > 0, \theta \in [0, 1]$ and $\mu > 0$, it is obvious that $\alpha > 0$.

(c) Substituting α in (D.1) and performing straightforward manipulation shows that (15a) holds. Since $\alpha > 0$, it holds that $\frac{\theta}{\mu \theta + \omega - \omega \theta} \geq 0$. The function $|\Delta^V(\theta)|$ is monotonically increasing for $\theta \in [0, 1]$. Furthermore, it is straightforward to obtain (16).

In steady state, $\mathbf{I}_c = \alpha (\theta \mathbf{I}_c^* + (1 - \theta) \mathbf{I}_{b_c})$. Therefore, we have $\mathbf{I}_c^{pu} = \alpha (\theta \mathbf{1}_N + (1 - \theta) \mathbf{I}_{b_c}^{pu})$, where

$\mathbf{I}_{b_c}^{pu} = \text{diag}(\mathbf{I}_c^*)^{-1} \mathbf{I}_{b_c}$. By Definition 1, we have $\mathbf{I}_c^{pu} = \mathbf{I}_{avg_c}^{pu} (\Delta^{I_c} + \mathbf{1}_m)$ with $\mathbf{1}_m^T \Delta^{I_c} = 0$. Consequently,

$$\mathbf{I}_{avg_c}^{pu} (\Delta^{I_c} + \mathbf{1}_m) = \alpha (\theta \mathbf{1}_m + (1 - \theta) \mathbf{I}_{b_c}^{pu}), \quad (\text{D.2})$$

which further implies, by left multiplying (D.2) by $\mathbf{1}_m^T$, that $\mathbf{I}_{avg_c}^{pu} = \alpha (\theta (1 - \bar{I}_{b_c}^{pu}) + \bar{I}_{b_c}^{pu})$, where $\bar{I}_{b_c}^{pu} = \frac{1}{m} \mathbf{1}_m^T \mathbf{I}_{b_c}^{pu}$. Hence, substituting $\mathbf{I}_{avg_c}^{pu}$ into (D.2) yields

$$\Delta^{I_c}(\theta) = \left(\frac{1}{\theta (1 - \bar{I}_{b_c}^{pu}) + \bar{I}_{b_c}^{pu}} - 1 \right) \frac{\bar{I}_{b_c}^{pu}}{1 - \bar{I}_{b_c}^{pu}} \Delta_b^{I_c}, \quad (\text{D.3})$$

where $\Delta_b^{I_c} = (\mathbf{I}_{b_c}^{pu} - \bar{I}_{b_c}^{pu} \mathbf{1}_m) / \bar{I}_{b_c}^{pu}$. It is straightforward to conclude that $\Delta^{I_c}(\theta)$ is monotonous on $\theta \in [0, 1]$. Moreover, letting $\theta = 1$ yields $\Delta^{I_c}(1) = 0$. Thus, $|\Delta^{I_c}(\theta)|$ is monotonically decreasing on $\theta \in [0, 1]$.

(d) According to (C.1), $\mathbf{I}_o = (\bar{\mathbf{Y}}_{22} - \mathbf{Y}_{21} \bar{\mathbf{Y}}_{11}^{-1} \mathbf{Y}_{12}) \mathbf{V}_o + \mathbf{Y}_{21} \bar{\mathbf{Y}}_{11}^{-1} \mathbf{I}_c$. Considering, in steady state, $\mathbf{I}_o = \alpha \mathbf{I}_o^*$ and $\mathbf{I}_c = \alpha (\theta \mathbf{I}_c^* + (1 - \theta) \mathbf{I}_{b_c})$, we have

$$\alpha (\mathbf{I}_o^* - \mathbf{Y}_{21} \bar{\mathbf{Y}}_{11}^{-1} (\theta \mathbf{I}_c^* + (1 - \theta) \mathbf{I}_{b_c})) = \bar{\mathbf{Y}}_{11} | \bar{\mathbf{Y}} \mathbf{V}_o.$$

Then, substituting α into the above equation yields $\mathbf{V}_o = \frac{1}{\theta \mu + \omega (1 - \theta)} (\theta \Omega_1 + \Omega_2)$. Furthermore, it is derived that each entry of \mathbf{V}_o is a monotone function for $\theta \in [0, 1]$, and $\mathbf{V}_o = \frac{1}{\theta (\mu - \omega) + \omega} (\Omega_2 - \frac{\omega}{\mu - \omega} \Omega_1) + \frac{1}{\mu - \omega} \Omega_1$.

E Proof of Proposition 2

(a) According to (16), it is trivial to obtain that $\theta_d = 1$ (or $\theta_d = 0$) if $\|\Delta^{V_c}(1)\|_\infty < \Gamma_V$ (or $\Gamma_V = 0$). Then, according to (15a) and considering $\mu \theta_d + \omega (1 - \theta_d) > 0$, for given Γ_V , if $\Gamma_V \in (0, \|\Delta^{V_c}(1)\|_\infty]$, it holds that $\Gamma_V = \max_\theta \|\Delta^{V_c}(\theta)\|_\infty = \frac{\theta_d}{(\mu - \omega) \theta_d + \omega} \|\Psi_1\|_\infty$, which further implies $\theta_d = \frac{\omega \Gamma_V}{\|\Psi_1\|_\infty - \Gamma_V (\mu - \omega)}$.

(b) The range of ω is determined by the admissible range of the output currents of DGs. According to the statement (a) of Theorem 1, in steady state, the output per-unit currents of DGs at critical nodes are $\mathbf{I}_c^{pu} = \frac{\theta}{\mu \theta + \omega (1 - \theta)} \mathbf{1}_m + \frac{1 - \theta}{\mu \theta + \omega (1 - \theta)} \text{diag}(\mathbf{I}_c^*)^{-1} \mathbf{I}_{b_c}$. Since $I_i^{pu} = \frac{I_i}{I_i^*} \geq 0, \forall i \in \mathcal{M}$, and $\mathbf{I}_{b_c} = \omega V_{rat} \bar{\mathbf{Y}}_{22} | \bar{\mathbf{Y}} \mathbf{1}_m + \mathbf{Y}_{12} \bar{\mathbf{Y}}_{22}^{-1} \mathbf{I}_o^*$, we have $(1 - \theta) (\omega V_{rat} \bar{\mathbf{Y}}_{22} | \bar{\mathbf{Y}} \mathbf{1}_m + \mathbf{Y}_{12} \bar{\mathbf{Y}}_{22}^{-1} \mathbf{I}_o^*) \geq -\theta \mathbf{I}_c^*$. Further considering $\bar{\mathbf{Y}}_{22} | \bar{\mathbf{Y}} \mathbf{1}_m \geq 0$ and $\bar{\mathbf{Y}}_{22} | \bar{\mathbf{Y}} \mathbf{1}_m \neq 0$ yields $\omega \in \left[\max_i \left\{ \frac{\zeta_i}{\nu_i} \right\}, +\infty \right), i \in \mathcal{M}_c, \forall \nu_i \neq 0$. where $[\zeta_1, \dots, \zeta_m]^T = \frac{-\theta}{1 - \theta} \mathbf{I}_c^* - \mathbf{Y}_{12} \bar{\mathbf{Y}}_{22}^{-1} \mathbf{I}_o^*, [\nu_1, \dots, \nu_m]^T = V_{rat} \bar{\mathbf{Y}}_{22} | \bar{\mathbf{Y}} \mathbf{1}_m$.

(c) Since $\mathbf{I}_o^{pu} = \frac{1}{\mu \theta + \omega (1 - \theta)}$, it is straightforward to show the monotonic decreasing property of \mathbf{I}_o^{pu} on $\omega \in \mathcal{W}$.

(d)

$\mathbb{1}_m^T \mathbf{I}_c = \frac{\theta}{\mu\theta + \omega(1-\theta)} \mathbb{1}_m^T \mathbf{I}_c^* + \frac{1-\theta}{\mu\theta + \omega(1-\theta)} \mathbb{1}_m^T \mathbf{I}_{b_c} = \eta_1 + \eta_2$,
 where $\eta_1 = \frac{(1-\theta)\omega V_{rat}}{\mu\theta + \omega(1-\theta)} \mathbb{1}_m^T \bar{\mathbf{Y}}_{22}^{-1} \bar{\mathbf{Y}} \mathbb{1}_m$, $\eta_2 = \frac{\theta \mathbb{1}_m^T \mathbf{I}_c^*}{\mu\theta + \omega(1-\theta)} + \frac{(1-\theta) \mathbb{1}_m^T \mathbf{Y}_{12} \bar{\mathbf{Y}}_{22}^{-1} \mathbf{I}_o^*}{\mu\theta + \omega(1-\theta)}$. Since $\theta \in [0, 1)$, $\mathbb{1}_m^T \bar{\mathbf{Y}}_{22}^{-1} \bar{\mathbf{Y}} \mathbb{1}_m > 0$ and $\mu > 0$, η_1 is monotonically increasing on $\omega \in \mathcal{W}$. Moreover, since $\mathbb{1}_m^T \mathbf{Y}_{12} \bar{\mathbf{Y}}_{22}^{-1} \mathbf{I}_o^* < 0$, η_2 is monotonically increasing on $\omega \in \mathcal{W}$ if $\theta \mathbb{1}_m^T \mathbf{I}_c^* + (1-\theta) \mathbb{1}_m^T \mathbf{Y}_{12} \bar{\mathbf{Y}}_{22}^{-1} \mathbf{I}_o^* < 0$. Thus, the monotonic increasing of $\mathbb{1}_m^T \mathbf{I}_c$ is established.

References

- Bai, H., Zhang, H., Cai, H., Schiffer, J., 2022. Voltage regulation and current sharing for multi-bus DC microgrids: a compromised design approach. *Automatica* 142, 110340.
- Caliskan, S.Y., Tabuada, P., 2014. Towards Kron reduction of generalized electrical networks. *Automatica* 50, 2586–2590.
- Che, L., Shahidehpour, M., 2014. DC microgrids: economic operation and enhancement of resilience by hierarchical control. *IEEE Transactions on Smart Grid* 5, 2517–2526.
- Cucuzzella, M., Trip, S., De Persis, C., Cheng, X., Ferrara, A., van der Schaft, A., 2018. A robust consensus algorithm for current sharing and voltage regulation in DC microgrids. *IEEE Transactions on Control Systems Technology* 27, 1583–1595.
- De Persis, C., Weitenberg, E.R., Dörfler, F., 2018. A power consensus algorithm for DC microgrids. *Automatica* 89, 364–375.
- Ding, L., Han, Q., Wang, L., Sindi, E., 2018. Distributed cooperative optimal control of DC microgrids with communication delays. *IEEE Transactions on Industrial Informatics* 14(9), 3924–3935.
- Dörfler, F., Bullo, F., 2013. Kron reduction of graphs with applications to electrical networks. *IEEE Transactions on Circuits and Systems I: Regular Papers* 60(1), 150–163.
- Dörfler, F., Simpson-Porco, J.W., Bullo, F., 2018. Electrical networks and algebraic graph theory: Models, properties, and applications. *Proceedings of the IEEE* 106, 977–1005.
- Dragičević, T., Lu, X., Vasquez, J.C., Guerrero, J.M., 2015. DC microgrids - Part I: A review of control strategies and stabilization techniques. *IEEE Transactions on Power Electronics* 31, 4876–4891.
- Han, R., Wang, H., Jin, Z., Meng, L., Guerrero, J.M., 2019. Compromised controller design for current sharing and voltage regulation in DC microgrid. *IEEE Transactions on Power Electronics* 34(8), 8045–8061.
- Kia, S.S., Van Scoy, B., Cortes, J., Freeman, R.A., Lynch, K.M., Martinez, S., 2019. Tutorial on dynamic average consensus: the problem, its applications, and the algorithms. *IEEE Control Systems Magazine* 39, 40–72.
- Lewis, F.L., Zhang, H., Hengster-Movric, K., Das, A., 2014. *Cooperative Control of Multi-Agent Systems: Optimal and Adaptive Design Approaches*. Springer, London.
- Liu, X., Wang, Y., Liu, Z., Huang, Y., 2023. On the stability of distributed secondary control for DC microgrids with grid-forming and grid-feeding converters. *Automatica* 155, 111164.
- Liu, Z., Li, J., Su, M., Liu, X., Yuan, L., 2024. Stability analysis of equilibrium of dc microgrid under distributed control. *IEEE Transactions on Power Systems* 39, 1058–1067.
- Nahata, P., Soloperto, R., Tucci, M., Martinelli, A., Ferrari-Trecate, G., 2020. A passivity-based approach to voltage stabilization in DC microgrids with ZIP loads. *Automatica* 113, 108770.
- Nahata, P., Turan, M.S., Ferrari-Trecate, G., 2022. Consensus-based current sharing and voltage balancing in DC microgrids with exponential loads. *IEEE Transactions on Control Systems Technology* 30, 1668–1680.
- Nasirian, V., Moayedi, S., Davoudi, A., Lewis, F.L., 2015. Distributed cooperative control of DC microgrids. *IEEE Transactions on Power Electronics* 30(4), 2288–2303.
- Prabhakaran, P., Goyal, Y., Agarwal, V., 2018. Novel nonlinear droop control techniques to overcome the load sharing and voltage regulation issues in DC microgrid. *IEEE Transactions on Power Electronics* 33(5), 4477–4487.
- Pratt, A., Kumar, P., Aldridge, T.V., 2007. Evaluation of 400v DC distribution in telco and data centers to improve energy efficiency, in: *Proc. of 29th International Telecommunications Energy Conference*, pp. 32–39.
- Schiffer, J., Zonetti, D., Ortega, R., Stankovic, A.M., Sezi, T., Raisch, J., 2016. A survey on modeling of microgrids: From fundamental physics to phasors and voltage sources. *Automatica* 74, 135–150.
- Shafiee, Q., Dragičević, T., Vasquez, J.C., Guerrero, J.M., 2014. Hierarchical control for multiple DC-microgrids clusters. *IEEE Transactions on Energy Conversion* 29, 922–933.
- Trip, S., Cucuzzella, M., Cheng, X., Scherpen, J., 2019. Distributed averaging control for voltage regulation and current sharing in DC microgrids. *IEEE Control Systems Letters* 3, 174–179.
- Tucci, M., Meng, L., Guerrero, J.M., Trecate, G.F., 2018. Stable current sharing and voltage balancing in DC microgrids: A consensus-based secondary control layer. *Automatica* 95, 1–13.